Evaluation of the dilatant behavior of a crystalline rock using full-field optical imaging and ultrasonic monitoring

Deepanshu Shirole
Department of Civil Engineering, IIT Delhi, New Delhi, India

Gabriel Walton
Department of Geology and Geological Engineering, Colorado School of Mines, Golden, USA

Ahmadreza Hedayat
Department of Civil and Environmental Engineering, Colorado School of Mines, Golden, USA

Sankhaneel Sinha
Department of Geology and Geological Engineering, Colorado School of Mines, Golden, USA

ABSTRACT: Experimental study of rock specimens under uniaxial stress path has shown that ultimate failure in rocks occurs after the onset of crack coalescence associated with dilatancy. Typically, rock dilatancy is represented by estimation of averaged specimen-scale total volumetric strains (ε_v). However, in previous studies, full-field ε_v (i.e. variations throughout a specimen) has not been rigorously analyzed. Accordingly, in this work, the full-field deformation measurement method of 2D-DIC (digital image correlation) is implemented to characterize evolution of dilatative ($\varepsilon_v < 0$) and contractive ($\varepsilon_v > 0$) strains in Stanstead granite specimens under uniaxial loads. In-sync, ultrasonic monitoring was also conducted to non-destructively monitor damage in the specimen. Results showed that full field ε_v strains evolve in a heterogeneous manner, with some regions showing dilation, and some showing contraction. Also, increases in ultrasonic amplitude during the initial stages of testing were shown to be linked to the occurrence of contractant strains.

Keywords: Image correlation, ultrasonic monitoring, dilatancy, contraction.

1 INTRODUCTION

Rock microstructure is typically represented by an assembly of heterogeneous mineral grains, which may vary in their mechanical (stiffness, hardness) and geometrical (size, shape) properties (Lan et al., 2010). This grain-scale heterogeneity contributes to the evolution of a heterogeneous strain/or stress field in the rock volume, causing locally extensile regions to originate even under a globally compressive stress-field (Diederichs, 2003a). Such localized strain and associated progressive damage can lead to an overall increase in the dilatancy (negative total volumetric strains, ε_v) of hard brittle rocks, which is consistent with the fact that crack nucleation and coalescence processes in rocks are typically followed by absolute or relative dilatancy (Cieślik, 2018; Diederichs, 1999; Shirole et al., 2019, 2020; Sinha & Walton, 2019). In previous studies, the evolution of ε_v (with stress) was estimated either through point-based surficial mechanical measurement systems (e.g., strain gauges) or via computation of the fluid displacements in the triaxial cells. Accordingly, the typical ε_v measurements are either representative of average strains acting on a small region present on the specimen surface or are an average of the strains distributed across the whole specimen.

Consequently, only scarce amount of information is available on the characteristics of full-field (across the specimen surface) strain evolution in brittle rocks, specifically in the context of total volumetric strains (ε_v). To bridge this knowledge gap, in this study, the non-contact optical displacement measurement method of 2D-DIC (digital image correlation) is implemented in combination with ultrasonic monitoring for near-continuous assessment of the evolution of full-field volumetric strains in a crystalline rock (Stanstead granite) under monotonic uniaxial loading. As DIC provides quantitative information on the temporal and spatial development of rock deformation under external loading, it can directly facilitate objective assessment of characteristics of volumetric strain development in rocks at various stages of damage and stress in the rock (Lin & Labuz, 2008). In addition, the ultrasonic parameters can provide information on the internal changes in the rock volume during loading. Specifically, in this study, the aim is to classify the contribution of dilatative (negative ε_v magnitude) and contractive (positive ε_v magnitude) regions in the rock volume on the evolution of total volumetric strains (ε_v). An attempt has also been made to demonstrate the heterogeneity in distribution of the ε_v at increasing stress levels. Note that while the data presented in this study corresponds to tests that have previously been analyzed (Shirole et al., 2020b, 2020a), the volumetric strain data as presented in this study have not previously been analyzed.

2 2D-DIGITAL IMAGE CORRELATION (2D-DIC)

2D-DIC serves as an automated platform for computation of full-field displacements and strains on a material surface (Hedayat & Walton, 2016). Typically, for computation of deformations (strains) through DIC, a quantitative comparison of specimen' digital images (procured at varying stages of loading) is performed based on correlation of the grey-scale intensities. Specifically, a reference image is initially selected, which is subsequently discretized into arrays of pixels, defined as subsets. Number of pixels in each subset is the 'subset size'. 2D-DIC computes deformation at the centre of subset (i.e., at DIC grid point, termed as 'elements') via a cross-correlation function. Analyzed displacements, when assembled, generate full-field displacement profile, which after spatial differentiation, provide full-field strains. Subsets are generally overlapped to enhance DIC accuracy, and overlapping distance is termed as 'step size' (Shirole et al., 2019b).

3 EXPERIMENTAL DESIGN AND METHODS

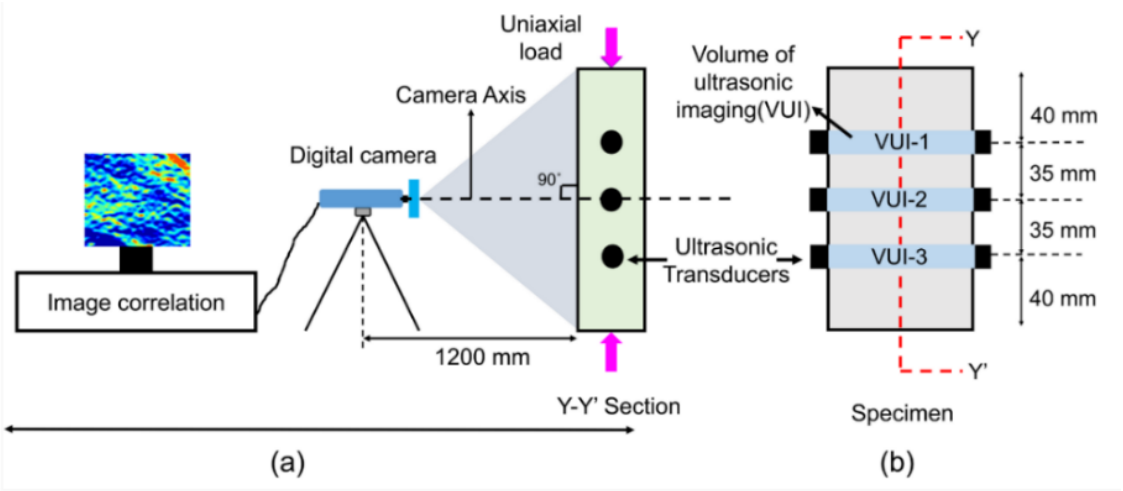

Figure 1. Schematic diagram of the experimental scheme employed in this study.

The study was carried out on Stanstead granite (SG) rock specimens. The grain size of SG varies between 0.5-2 mm, and the rock consists of a mix of feldspar (~65%), biotite (~8.5%) and quartz (~25%) (Shirole et al., 2020). The average uniaxial compressive strength of SG is 140 MPa, with crack initiation (CI) and crack damage (CD) threshold of ~40% and ~78% of UCS, respectively

(Shirole et al., 2019b). For uniaxial tests performed in displacement control at 1 μm/s, prismatic-shaped specimens (150×75×25 mm, Figure 1) were employed to ensure a planar surface.

During the uniaxial tests, digital images of the entire specimen surface were acquired in real-time using a Grasshopper camera system (Figure 1). The camera was mounted at 1.2 m (z_c) from the specimen to ensure minimum distortion. The resolution of the imaging was 80 μm per pixel. Furthermore, subset and step sizes were selected to be 12 and 5 pixels, respectively. Critically, a random pattern of gray-scale intensities was generated on the specimen using RustOleum, which ensured unique subset identification - a requirement for accurate DIC mapping (Shirole et al., 2020).

Concurrent to image capturing, ultrasonic measurements were carried out at three locations on the specimen surface (Figure 1). For maximum ultrasonic sensitivity, transducers were placed normal to the load direction (Shirole et al., 2020). To improve acoustic impedance, honey was used as the coupling medium between rock and transducer. Compressional transducers (1 MHz, and 13 mm diameter) from Olympus NDT, Inc. were used as the source/receiver of the ultrasonic signals. For generation of ultrasonic signals, a negative square waveform generator from Olympus NDT, Inc. was used. For the digitization of acquired ultrasonic signals, a LabVIEW-based multi-channel fast ultrasonic system was used at a sampling frequency of 100 MHz (for details, refer to Shirole, 2019).

From the image correlated full-field strains, total volumetric strain ($\varepsilon_{v,i}$), at each of the individual DIC element (i), was computed using Equation 1 (Ghazvinian, 2015):

$$\varepsilon_{v,i} = \varepsilon_{a,i} + 2 \cdot \varepsilon_{x,i} \tag{1}$$

where, $\varepsilon_{x,i}$ and $\varepsilon_{a,i}$ are the lateral and axial strains at the individual DIC elements. As the specimen thickness is relatively small (~25 mm), the specimens are effectively under plane stress conditions. Consequently, the out-of-plane strains ($\varepsilon_{z,i}$) are expected to be similar to the lateral strains ($\varepsilon_{x,i}$), and they are assumed to be equal (due to macroscopic isotropy) in Equation 2. For evaluation of 'mean' total volumetric strain ($\varepsilon_{v,m}$), the $\varepsilon_{v,i}$ magnitude across all the DIC elements (N=57270) was averaged at each load increment. Additionally, the number of dilatative elements (DE; $\varepsilon_{v,i}$<0) and contractive elements (CE; $\varepsilon_{v,i}$>0) evolving in the rocks specimens during tests were also computed. The normalized dilatative (NDE) and contractive elements (NDE) were computed as the ratio of DE or CE to the total DIC elements (N), respectively. Furthermore, for evaluation of the contractive (CVS) and dilatative (DVS) components of $\varepsilon_{v,m}$, Equation 2 was utilized:

$$CVS = \frac{1}{CE}\sum_{i=1}^{CE}(\varepsilon_{v,i}) \text{ , for } \varepsilon_{v,i} > 0$$

$$DVS = \frac{1}{DE}\sum_{i=1}^{DE}(\varepsilon_{v,i}) \text{ , for } \varepsilon_{v,i} < 0 \tag{2}$$

Furthermore, to characterize the progression of tensile damage (ε_{AT}^{NE}), a strain metric similar to that was implemented by Shirole et al. (2020) was employed:

$$\varepsilon_{AT}^{NE} = \sum_{i=1}^{N} \varepsilon_{33,i} \text{ , for } \varepsilon_c > \varepsilon_{33,i} \tag{3}$$

where, $\varepsilon_{33,i}$ is the minor principal strain at the individual DIC elements.

4 RESULTS AND DISCUSSION

The ultrasonic signals acquired at various stages of the applied loading is shown in Figure 2. Modulations in amplitude of ultrasonic signals (with percent failure stress) measured at three VUIs (Figure 2). It broadly shows that amplitude variations are fairly consistent for the three VUIs. In particular, at initial stress levels (up to ~30-35% of UCS), ultrasonic amplitude increases due to crack closure effects. With subsequent stress, the rate of increase in amplitude attenuates, which is associated with evolution of damage in the rock, as damage acts as a low-pass filter. Around ~70-

80% of UCS, amplitude shows an accelerated rate of attenuation as CD threshold is exceeded, which tends to increase rock dilation, reducing signal transmission (Shirole et al., 2020b).

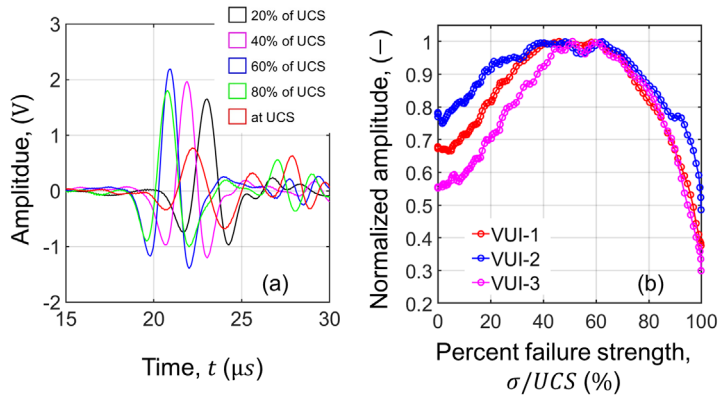

Figure 2. Variation of ultrasonic wave amplitude as a function of stress.

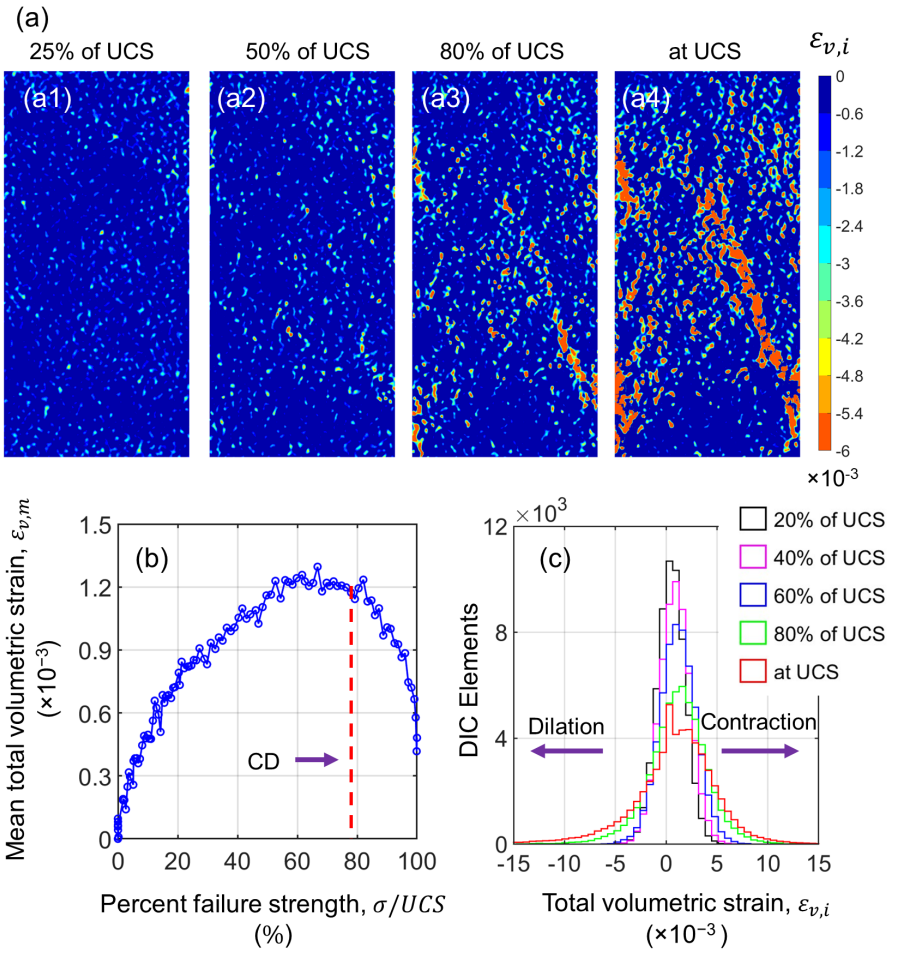

Figure 3. (a) Full-field strain maps of the total volumetric strain (ε_v), (b) evolution of mean total volumetric strain ($\varepsilon_{v,m}$), and (c) histogram of ε_v distribution across the DIC elements.

Figure 3a shows full-field maps of $\varepsilon_{v,i}$ strains as it evolves with applied stress. These maps particularly show regions of strain localization (heterogeneity), whose intensity increases with the magnitude of applied stress. Also, the regions of strain concentrations are fairly oriented sub-parallel

to stress direction, consistent with the fact that rock dilates primarily normal to applied stress field. Mean $\varepsilon_{v,\mathrm{m}}$ values were also computed at increasing loads (Figure 3b). It showed increasing $\varepsilon_{v,\mathrm{m}}$ magnitudes increase with loading (up to ~60% of UCS), suggesting that contraction fairly dominates specimen behavior up to this stress. With further increase in stress (i.e., around CD), $\varepsilon_{v,\mathrm{m}}$ shows a point of inflection, subsequent to which $\varepsilon_{v,\mathrm{m}}$ magnitude reduces, which is typically associated with onset of absolute dilatation (CD) (Diederichs, 2003). Noticeably, the magnitude of $\varepsilon_{v,\mathrm{m}}$ is positive (contractive, $\varepsilon_v > 0$) throughout the stress history (Figure 3b), in contrast, $\varepsilon_{v,i}$ strain maps are heterogeneous and explicitly indicate regions which undergo dilation ($\varepsilon_v < 0$, Figure 3a). For a quantitative investigation of heterogeneity in $\varepsilon_{v,i}$ evolution, distribution of $\varepsilon_{v,i}$ across the DIC elements was plotted (Figure 3c), which conspicuously indicate the even at low stress levels, rock elements experience both dilation and contraction (even under a global compressive strain field). Critically, at high stress levels, $\varepsilon_{v,i}$ distribution becomes relatively more dispersed (with higher contraction/dilation magnitudes) compared to low stress levels, which can be associated with damage accumulation and dilatancy in rock volume with application of stress.

Additionally, contractive (NCE) and dilatative (NDE) elements (normalized with respect to total DIC elements) evolving during the stress loading were also analyzed (Figure 4a). During the initial loading phase, NCE increases, while the NDE decreases (consistent with ultrasonic modulations shown in Figure 2b). In contrast, during the later stages of loading, NCE decreases (and NDE correspondingly increases). Notably, the proportion of CE remains higher than DE, throughout the testing duration. The magnitude of the ratio of DE to CE (i.e., <1, Figure 4b) further illustrates this. Around ~80% of UCS (CD), DE/CE ratio begins to increase at an accelerated rate with stress, marking progression of overall dilatancy in the rock volume (consistent with Figure 4a).

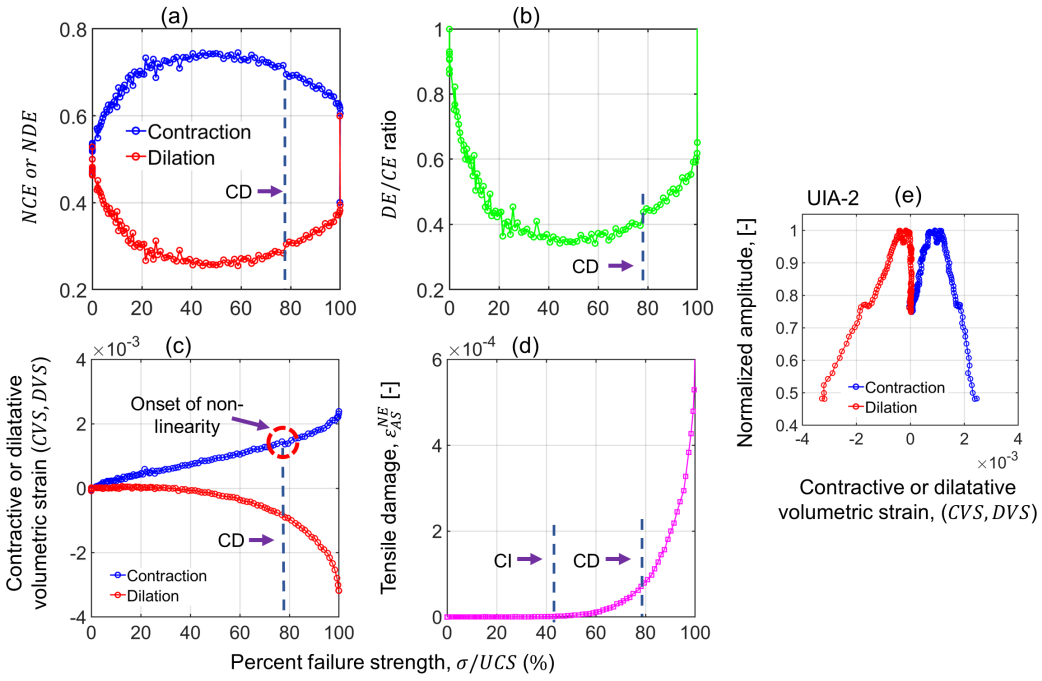

Figure 4. (a) Normalized (with respect to total elements) contractive (NCE) or dilatative (NDE) elements, (b) DE to CE ratio, (c) CVS and DVS, (d) tensile damage (e) correlation between amplitude and CVS/DVS.

Progression of contractive (CVS) and dilatative (DVS) volumetric strains were also tracked during the loading history (Figure 4c). CVS magnitude shows monotonic increase in its magnitude with the applied stress. In contrast, DVS shows only minor modulations during the early loading phase (up to ~40% of UCS) – indicating that rock dilatation is negligible at low levels of loading. With increasing stress, the DVS magnitude begin to increase (NDE also begins to amplify around the same stress magnitude) (Figure 4a). This increase in DVS values is associated with the extensile strain induced cracking processes (i.e., CI) in the rock specimen (Figure 4d). At around ~80% of UCS, DVS shows an accelerated rate of progression, which is indicative of absolute dilatancy in the rock volume. This

higher rate of increase in the DVS values are consistent with accelerated increase in the tensile damage magnitude (i.e., CD) around the same stress threshold (Figure 4d), suggesting that higher tensile damage leads to higher dilation in the rock volume.

Interestingly, non-linearity in the CVS vs. stress curve was observed around the CD threshold (Figure 4c), suggesting that around CD, the CVS magnitude shows higher rate of increase for a unit change in stress. The increase in CVS is synchronous to the increase in DVS – suggesting that dilation and contraction both increase around CD. This suggests that around CD, as the dilation increases in the rocks, it leads to amplification in the contractive strains (dilation-induced contraction). Additionally, visual inspection of the slopes of ultrasonic amplitude curves in Figure 4e suggests that ultrasonic amplitude is more sensitive to dilative strain (DVS) during attenuation, relative to contractive strains (CVS) (Figure 4e). In contrast, ultrasonic amplitude amplification during initial stages of testing is more sensitive to CVS relative to dilatative strains, which are nearly constant during this phase of testing.

5 CONLUSIONS

A 2D-DIC procedure was implemented to explicitly analyze the full-field volumetric strains in Stanstead granite rock. The results show that volumetric strains are heterogeneously dispersed with contractive and dilatative elements. At low-levels of loading, the dilation in the rock elements is negligible, which subsequently increases close to the ultimate failure of the rock. Interestingly, increasing tensile damage leads to higher dilation in the rock volume. Higher dilatation around CD also causes onset of non-linearity in the contractile strains. Also, ultrasonic amplitude amplification at initial load levels is shown to be more sensitive to contractive strains relative to dilatative strains.

6 REFERENCES

Cieślik, J. (2018). Dilatancy as a measure of fracturing development in the process of rock damage. *Open Geosciences*, *10*(1), 484–490. https://doi.org/10.1515/geo-2018-0038

Diederichs, M. S. (1999). *Instability of hard rockmasses: The role of tensile damage and relaxation* [Ph.D. Thesis]. University of Waterloo, Cananda

Diederichs, M. S. (2003a). Manuel Rocha Medal Recipient Rock Fracture and Collapse Under Low Confinement Conditions. *Rock Mechanics and Rock Engineering*, *36*(5), 339–381.

Diederichs, M. S. (2003b). Manuel Rocha Medal Recipient Rock Fracture and Collapse Under Low Confinement Conditions. *Rock Mechanics and Rock Engineering*, *36*(5), 339–381.

Ghazvinian, E. (2015). *Fracture initiation and propagation in low porosity crystalline rocks: Implications for excavation damage zone (EDZ) mechanics* [Ph.D. Thesis]. Queen's University.

Hedayat, A., & Walton, G. (2016). Laboratory Determination of Rock Fracture Shear Stiffness Using Seismic Wave Propagation and Digital Image Correlation. *Geotechnical Testing Journal*, *40*(1).

Lan, H., Martin, C. D., & Hu, B. (2010). Effect of heterogeneity of brittle rock on micromechanical extensile behavior during compression loading. *Journal of Geophysical Research*, *115*(B1), B01202.

Shirole, D., Hedayat, A., & Walton, G. (2019). Experimental Relationship Between Compressional Wave Attenuation and Surface Strains in Brittle Rock. *Jour. of Geoph. Res.: Solid Earth*, *124*(6).

Shirole, D., Hedayat, A., & Walton, G. (2020b). Illumination of Damage in Intact Rocks by Ultrasonic Transmission-Reflection and Digital Image Correlation. *Jour. of Geoph. Res.: Solid Earth*, *125*(7).

Shirole, D., Hedayat, A., & Walton, G. (2019b). Influence of strain resolution on experimental correlation between ultrasonic amplitude and surface strains. *Proceedings of the 2020 International Symposium on Rock Mechanics and Rock Engineering*, 1–8.

Shirole, D., Walton, G., & Hedayat, A. (2020a). Experimental investigation of multi-scale strain-field heterogeneity in rocks. *International Journal of Rock Mechanics and Mining Sciences*, *127*, 104212.

Sinha, S., & Walton, G. (2019). Understanding continuum and discontinuum models of rock-support interaction for excavations undergoing stress-induced spalling. *Int. J. of Rock Mech.& Min. Sc.*, 104089.